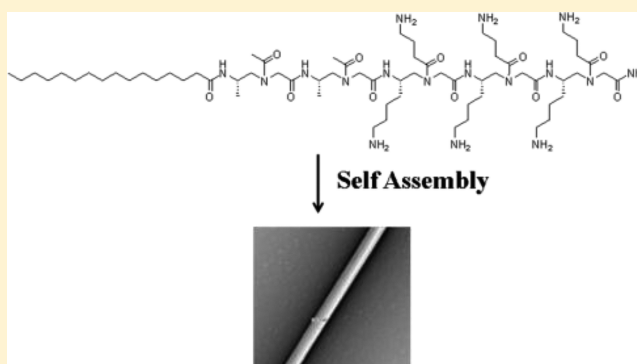


## Nanorods Formed from a New Class of Peptidomimetics

Youhong Niu,<sup>†</sup> Haifan Wu,<sup>†</sup> Rongfu Huang,<sup>†</sup> Qiao Qiao,<sup>†</sup> Frankie Costanza,<sup>†</sup> Xi-Sen Wang,<sup>†</sup> Yaogang Hu,<sup>†</sup> Mohamad Nassir Amin,<sup>†</sup> Anh-My Nguyen,<sup>†</sup> James Zhang,<sup>†</sup> Edward Haller,<sup>‡</sup> Shengqian Ma,<sup>†</sup> Xiao Li,<sup>†</sup> and Jianfeng Cai<sup>\*,†</sup><sup>†</sup>Department of Chemistry, University of South Florida, 4202 E. Fowler Ave., Tampa, Florida 33620, United States<sup>‡</sup>Department of Integrative Biology, University of South Florida, 4202 E. Fowler Ave., Tampa, Florida 33620, United States

## Supporting Information

**ABSTRACT:** Although peptide amphiphiles have been explored as nanomaterials for different applications, nanostructures formed by hierarchical molecular assembly of sequence-specific peptidomimetics are much less developed. Such protein-like nanomaterials could enhance the current application of peptide-based amphiphiles by enriching the diversity of nanostructures, increasing *in vivo* stability for biomedical applications, and facilitating the understanding of biomacromolecular self-assembly. Herein we present a biomimetic  $\gamma$ -AApeptide amphiphile which forms nanorods. Our results demonstrate the capability of  $\gamma$ -AApeptide amphiphiles as a potential scaffold for the preparation of biomimetic and bioinspired nanostructures. The programmability and biocompatibility of  $\gamma$ -AApeptides could lead to novel nanomaterials for a wide variety of applications.



## INTRODUCTION

Molecular self-assembly is ubiquitous and vitally important in nature. Through noncovalent interactions, monomeric units self-assemble together to construct complex systems with unique biological functions.<sup>1</sup> Examples of such hierarchical molecular assembly found in nature include self-assembly of lipids, proteins, and nucleic acids.<sup>2</sup> Research on molecular self-assembly is critical in nanotechnology because it sheds light on the understanding of molecular assembly mechanisms, the design of building blocks and monomeric units, and the construction of nanostructures and nanomaterials with desired functions.<sup>3</sup> There has been extensive interest in the development of peptide-based nanomaterials in the past decade, and their applications as nanomaterials, nanotechnology, and nanomedicines have been widely explored.<sup>3</sup> In these cases, polypeptides are used as monomer units to self-assemble into ordered nanostructures so as to develop novel functional nanobiomaterials that can mimic protein structures and functions.<sup>4,5</sup> This is because there are 20 natural amino acids that can be used as building blocks to construct an enormous number of peptides and proteins with a wide variety of lengths, hydrophobicity/hydrophilicity, and shapes, which leads to the formation of different nanostructures through self-assembly.<sup>3</sup> Among these peptide-based nanomaterials, peptide amphiphiles are mostly used to generate self-assembled nanostructures in aqueous environment.<sup>6</sup> Peptide amphiphiles consist of a hydrophilic peptide head with desired structures and functions and a hydrophobic tail. In aqueous solution, the hydrophobic tail, normally an alkyl chain, lipid, or hydrophobic peptide,

induces the aggregation of peptide amphiphiles. Meanwhile, the hydrophilic heads, consisting of polar or charged amino acid residues, assemble into nanostructures through hydrophilic interactions with water and other molecules. So far, the nanostructures generated by peptide amphiphiles include nanotubes, nanorods, nanovesicles, micelles, nanobelts, and nanofibers.<sup>7–13</sup>

However, despite tremendous effort in the development of peptide-based nanomaterials, non-natural oligomeric peptidomimetic-based nanomaterials have been much less explored.<sup>14–16</sup> Investigation of non-natural oligomer-based nanomaterials could theoretically lead to novel biomimetic and bioinspired materials with improved stability *in vivo* than peptide-based materials for biological applications. In the meantime, research can enrich the diversity of peptide-based nanomaterials by discovering novel nanostructures, as seen for those reported peptoid<sup>15,16</sup> and  $\beta$ -peptide-based nanomaterials.<sup>14</sup> Lastly, the development of peptidomimetic-based nanomaterials could lead to a better understanding of mechanism and motif of molecular self-assembly and artificial protein structures and functions.

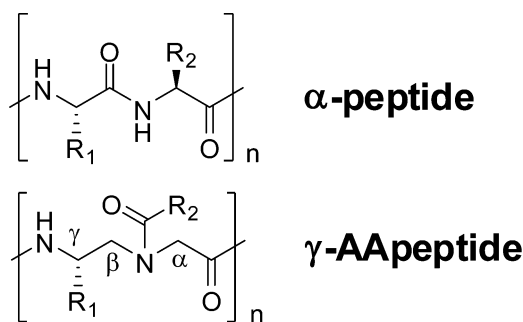
We have recently developed a new class of peptidomimetics termed " $\gamma$ -AApeptides".<sup>17,18</sup> As shown in Scheme 1,  $\gamma$ -AApeptides contain identical numbers of side chains to regular peptides of same lengths. However, compared to  $\alpha$ -peptides,

Received: July 29, 2012

Revised: August 31, 2012

Published: September 7, 2012

**Scheme 1. Representative Structure of a Conventional  $\alpha$ -Peptide and a  $\gamma$ -AApeptide**



AApeptides are much more diverse since a wide variety of side chains can be introduced through acylation. AApeptides are currently finding their application biomedical sciences.<sup>17–26</sup> Herein, for the first time, we show a biomimetic  $\gamma$ -AApeptide amphiphile which forms giant nanorods through hierarchical molecular self-assembly by mimicking the assembly motif of peptide amphiphiles. The nanostructure represents novel architectures that can be developed for material and biological applications. Our results suggest that the programmability and biocompatibility of  $\gamma$ -AApeptides could lead to a new class of nanomaterials for a wide variety of applications.

## EXPERIMENTAL SECTION

**General Experimental Methods.** Fmoc-protected  $\alpha$ -amino acids and Rink amide resin were obtained from Chem-Impex International, Inc. All other reagents and solvents were provided by either Sigma-Aldrich or Fisher Scientific. NMR spectra of intermediates and  $\gamma$ -AApeptide building blocks were obtained on a Varian Inova 400.  $\gamma$ -AApeptide amphiphiles were prepared on a Rink amide resin in peptide synthesis vessels on a Burrell Wrist-Action shaker. The  $\gamma$ -AApeptide amphiphiles were analyzed and purified on an analytical and a preparative Waters HPLC systems, respectively, and then lyophilized using a Labcono lyophilizer. Molecular weights of  $\gamma$ -AApeptides were identified on a Bruker AutoFlex MALDI-TOF mass spectrometer. TEM images were obtained on a FEI Morgagni 268D TEM with an Olympus MegaView III camera on the microscope.

**Solid Phase Synthesis, Purification, and Characterization of  $\gamma$ -AApeptide Amphiphiles.**<sup>21,22,24</sup>  $\gamma$ -AApeptide amphiphiles were prepared on a Rink amide resin in peptide synthesis vessels on a Burrell Wrist-Action shaker following the standard Fmoc chemistry of solid phase peptide synthesis protocol. Each coupling cycle included an Fmoc deprotection using 20% piperidine in DMF and 4 h coupling of 1.5 equiv of  $\gamma$ -AApeptide building blocks onto resin in the presence

of 2 equiv of DIC (diisopropylcarbodiimide)/oxohydroxybenzotriazole in DMF. After desired sequences were assembled, they were transferred into a 4 mL vial and cleaved from solid support in 74:24:2 TFA/ $\text{CH}_2\text{Cl}_2$ /triisopropylsilane for 2 h. Then solvent was evaporated, and the residues were analyzed and purified on an analytical (1 mL/min) and a preparative Waters (20 mL/min) HPLC systems, respectively. Both HPLC had same methods which were using 5% to 100% linear gradient of solvent B (0.1% TFA in acetonitrile) in A (0.1% TFA in water) over 40 min, followed by 100% solvent B over 10 min. The desired fractions were collected and lyophilized. The molecular weights of  $\gamma$ -AApeptide amphiphiles were obtained on Bruker AutoFlex MALDI-TOF mass spectrometer using  $\alpha$ -cyano-4-hydroxycinnamic acid as the matrix.

**Typical Procedure for Preparation of Grids and TEM Study.** The samples were applied to TEM grids by adding a 10  $\mu\text{L}$  sample solution, and the grids were allowed to dry for about 1 h. After being dried, the grids were stained with 10  $\mu\text{L}$  of 1% (w/w) uranyl acetate aqueous solution, and extra solution was removed by immersion using wet filter paper after 30 s. The grids were again allowed to dry for TEM study. TEM images were obtained on a FEI Morgagni 268D TEM with an Olympus MegaView III camera on the microscope. The microscope uses AnalySiS software to run the camera. The microscope was operated at 60 kV.

**Raman Spectroscopy.** All Raman experiments were carried out using a confocal Raman microscope (LabRam Horiba Jovin Yvon) equipped with a notch Rayleigh rejection filter, a 600 lines/mm diffraction grating, and a cooled CCD detector. Radiation at 514 nm wavelength from an argon and krypton laser (Coherent, Innova 70C series) was applied. After the laser beam passed through a laser filter monochromator, the power incident on the sample was around 50 mW. A 20 $\times$  objective was used throughout the experiments which yields a spot diameter of less than 5  $\mu\text{m}$  of the sample. In order to obtain high-quality Raman spectra, both the exposure time and accumulation time were varied. The Raman spectra were measured in the frequency range from 200 to 3600  $\text{cm}^{-1}$ .

**Mineralization of  $\text{CaCO}_3$ .**  $(\text{NH}_4)_2\text{CO}_3$  vapor was diffused into a 96-well plate, in which one well contained 198  $\mu\text{L}$  of 5.0 mM  $\text{CaCl}_2$  solution and 2  $\mu\text{L}$  of 1 mg/mL  $\gamma$ -AA1, giving a final concentration of 10  $\mu\text{g}/\text{mL}$ . The control did not contain  $\gamma$ -AA1; instead, 2  $\mu\text{L}$  of water was added. The 96-well plate was placed in a closed Ziploc bag for 3 days to allow  $(\text{NH}_4)_2\text{CO}_3$  vapor diffusion. The morphology of crystals was investigated by optical microscopy.

## RESULTS AND DISCUSSION

Similar to self-assembly of peptide amphiphiles, which are dominated by hydrogen bonding, hydrophobic, and electrostatic interactions,<sup>3</sup> we designed a  $\gamma$ -AApeptide amphiphile  $\gamma$ -AA1 that contains a hydrophilic head, a hydrophobic buffer region, and a C16 alkyl chain tail (Figure 1). The hydrophobic buffer region is introduced here to increase the hydrophobicity

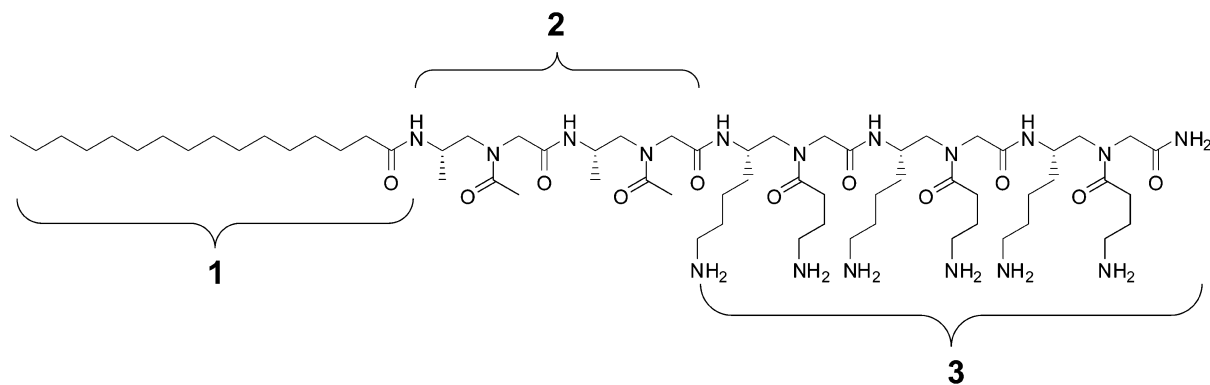


**Figure 1.** Design of  $\gamma$ -AApeptide amphiphile  $\gamma$ -AA1. Region 1 is the hydrophobic C16 alkyl tail, region 2 is the hydrophobic buffer region, and region 3 is the positively charged head.

and therefore to further enhance the capability of aggregation of the  $\gamma$ -AApeptide amphiphile in water solution. On the other hand, this region also increases the flexibility of hydrophilic head groups and optimizes the electrostatic interactions between head groups.

$\gamma$ -AA1 was found to be very soluble in water under experimental conditions. The unique self-assembled structure was observed after 7 days by transmission electron microscopy (TEM) using negative stain (uranyl acetate) and AFM. Both TEM and AFM reveal unprecedented giant nanorods dominant in aqueous solution at a concentration of 0.05 wt % (Figure 2).

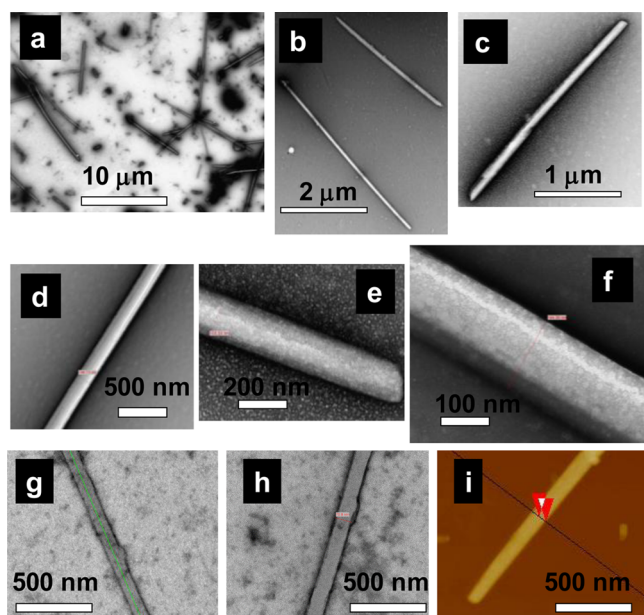


**Figure 2.** Giant nanorods assembled from the  $\gamma$ -AApeptide amphiphile  $\gamma$ -AA1 in water (0.5 mg/mL) after 7 days. (a–h) TEM images (negative uranyl acetate staining) of  $\gamma$ -AApeptide nanorods. (a) shows the abundance of nanorods within one sample. The dark spots in (a) are artifacts from the uranyl acetate stain. (b–f) Nanorods at different scanning sizes. (g) Nanorods in pH 4. (h) Nanorods in pH 10. (i) AFM image of a nanorod.

Compared to previously reported peptide nanorods,<sup>8</sup> which are only 3 nm in diameter and less than 100 nm in length, nanorods formed from the self-assembly of the  $\gamma$ -AApeptide amphiphile  $\gamma$ -AA1 are much larger. They have fairly monodisperse diameters of 100–200 nm and lengths of 2–10  $\mu$ m. This is consistent with the measurement of dynamic light scattering (DLS), which shows an average of diameter of 152 nm. These nanorods have highly ordered shapes and are stiff and straight, with a smooth and reflective surface. The morphology is distinct and does not resemble that of peptide nanorods. The nanorods are fairly stable in a wide pH range of 4–10 (Figure 2g,h). Such giant nanorods may provide a novel platform for nanocatalysis or nanomedicine by the introduction of proper functional epitopes.

The formation of nanostructure is also supported by Raman spectra (Figure 3). Figure 3 shows the typical Raman spectra of  $\gamma$ -AA1 (black: solid; red: in aqueous solution at room temperature). In the region of 2800–3000  $\text{cm}^{-1}$ , these peaks are assigned to the stretching mode of  $\text{CH}_3$ ,  $\text{CH}_2$ , and  $\text{CH}$ , respectively.<sup>27–29</sup> Above 3000  $\text{cm}^{-1}$ , the solid sample shows two weak vibrational peaks at 3280 and 3420  $\text{cm}^{-1}$  which can be assigned to the stretching mode of  $\text{NH}$  and  $\text{NH}_2$ . However, the

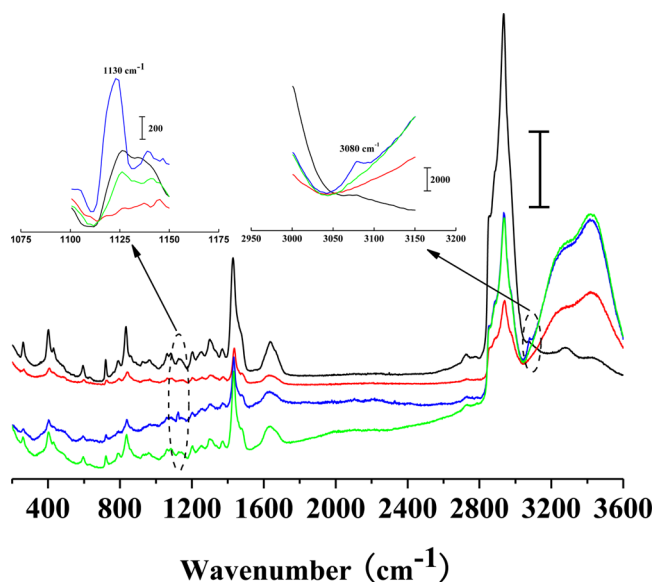


**Figure 3.** Typical Raman spectra of  $\gamma$ -AA1 nanorod in the range from 200 to 3600  $\text{cm}^{-1}$ . Top down: solid (black); aqueous solution at room temperature (red); aqueous solution at 60  $^{\circ}\text{C}$  (blue); aqueous solution cooled down after heat (green). The exposure time for solid is 1 s and 3 s for the other three aqueous solution samples. Scale bar:  $10^4$ . Inset: the expanded views of Raman spectra in the range of 1100–1150 and 3000–3150  $\text{cm}^{-1}$ .

two strong peaks in aqueous solution should be assigned to the symmetrical and asymmetrical stretching mode of OH band.

When the aqueous solution was heated to 60  $^{\circ}\text{C}$ , appealing spectra changes were observed when compared with that at room temperature, shown in Figure 3 (blue curve). Especially, the peaks at 406, 1090, 1305, and 1475  $\text{cm}^{-1}$  shifted to 402, 1085, 1300, and 1480  $\text{cm}^{-1}$ , which belong to the torsion mode of C–C chain, rocking mode of  $\text{CH}_3$ , and bending mode of  $\text{CH}$  and  $\text{CH}_2$ , respectively.<sup>27–29</sup> Also, 265, 480, 598, and 1145  $\text{cm}^{-1}$  shifted to 260, 470, 594, and 1138  $\text{cm}^{-1}$ , which can be assigned to the bending mode of C–C–N chain, rocking mode of carboxylic residue, bending mode of  $\text{C}=\text{O}$ , and torsion of  $\text{NH}_2$  at the hydrophilic head of  $\gamma$ -AA1. For these peaks, around 5  $\text{cm}^{-1}$  of the red-shift was observed when heated at 60  $^{\circ}\text{C}$ . These changes may indicate the conformation of nanostructures have changed at high temperature.

Additionally, two new peaks at 1123 and 3080  $\text{cm}^{-1}$  were observed at high temperature as indicated by arrows, which were assigned to the rocking and stretching mode of  $\text{NH}_3^+$ . This may be due to the increased exposure of amino groups at high temperature after the disruption of nanorods. Furthermore, the spectra of the sample cooled down from 60  $^{\circ}\text{C}$  (green curve) showed some differences when compared with the unheated one (red curve), which may indicate that the unique nanostructure was destroyed to a certain extent at high temperature, and it needs a certain amount of time to re-form the nanostructure. The findings are consistent with our observation that nanorods are formed after a few days. Taken together, the changes in Raman investigation show that there are weak interactions when the nanorod formed by self-assembly of  $\gamma$ -AA1, including both hydrophobic interactions between hydrophobic alkyl tails and the hydrophilic interactions between hydrophilic heads. This is also supported by CD spectra (Figure S2), in which the heated  $\gamma$ -AA1 shows no peaks (Figure S2A). However, after annealing for 7 days, an

intense negative peak is observed (Figure S2B). It suggests that in the nanorods  $\gamma$ -AA1 forms more defined structures, most likely extended conformations, similar to what has been observed previously.<sup>22</sup>

To further evaluate the weak interactions existing in nanorods, NMR was carried by dissolving  $\gamma$ -AA1 in D<sub>2</sub>O and measuring repeatedly over 10 days. However, no obvious changes were detected (Figure 4), indicating the molecular

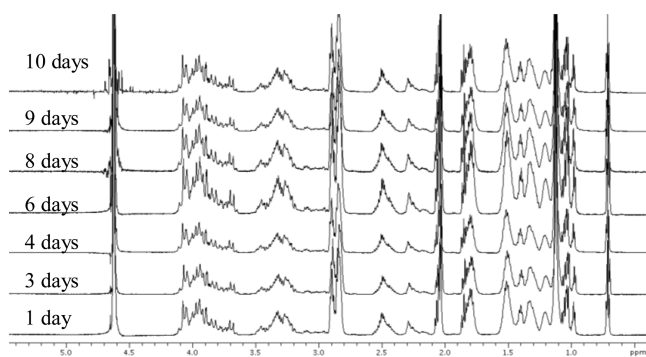


**Figure 4.** NMR spectra of  $\gamma$ -AA1 in D<sub>2</sub>O.

interactions in the nanorods are fairly subtle. Similar results were also observed using WXR (wide-angle X-ray diffraction). Solid obtained through lyophilization of  $\gamma$ -AA1 water solution after 7 days showed no difference from the original powder, and none of them show any peaks, an indication of amorphous nature (data not shown). This is also consistent with the unique backbone of  $\gamma$ -AApeptides, which do not form identical  $\beta$ -sheet structures that are normally identified in peptide amphiphiles. However, the results demonstrate that well-defined structures can still be formed through self-assembly of non-natural peptidomimetics through hydrophobic and hydrophilic interactions, even when each individual molecule does not have secondary structure similar to regular peptides.

The propensity to form such giant nanorods is high since the nanostructures are observed in water solution ranging from 0.02 to 1 mg/mL under the tested experiment conditions (CMC = 0.02 mg/mL). However, at 0.02 mg/mL concentration, the majority of the nanostructures are nanoparticles with diameters of 50–100 nm (Figure 5a), although nanorods

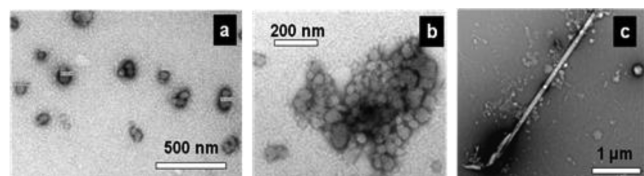


**Figure 5.** Morphology of nanostructures from the  $\gamma$ -AApeptide amphiphile  $\gamma$ -AA1 in water (0.02 mg/mL) after 7 days: (a) TEM images (negative uranyl acetate staining) of  $\gamma$ -AApeptide nanoparticles; (b) aggregated nanoparticles; (c) a growing nanorod is being appended with a short segment.

were still detected at such low concentrations (Figure 5c). Figure 5c clearly shows that the nanorod is elongated by joining with a shorter segment. It is also found that the nanoparticles tend to aggregate (Figure 5b) together even under this low concentration. Nanorods become dominant when concentration is higher than 0.1 mg/mL.

On the basis of these observations, we hypothesize that nanorods formed from the self-assembly of  $\gamma$ -AApeptide amphiphile  $\gamma$ -AA1 are formed by a hierarchical and dynamic process.  $\gamma$ -AA1 tends to first form vesicles (Figure 6). However,

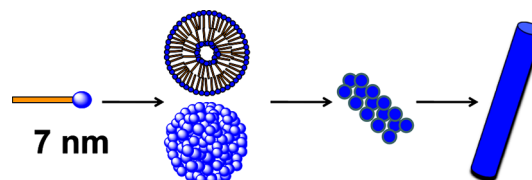


**Figure 6.** Schematic representation of nanorods formation from self-assembly of  $\gamma$ -AA1. The  $\gamma$ -AApeptide amphiphiles (hydrophobic tail colored in yellow and hydrophilic head colored in blue) first assemble into nanovesicles, which assemble and stack further to form giant nanorods.

such vesicles are unstable because  $\gamma$ -AA1 has multiple positively charged amino head groups, which lead to strong electrostatic repulsion when exposing to water. Therefore, these vesicles could gradually aggregate and stack together to form nanorods, where most of the amino groups can be buried inside, which can decrease electrostatic repulsion and increase hydrogen bonding among those amino groups. However, it is more likely that these spherical vesicles are resolved in the thermodynamic formation of nanorods. The detailed mechanisms are currently under investigation.

To test if the head groups are critical for the formation of nanorods, we prepared another  $\gamma$ -AApeptide amphiphile  $\gamma$ -AA2 (Figure 7), in which three amino groups in the hydrophilic head are removed and replaced with hydrophobic isopropyl groups. Self-assembly of this  $\gamma$ -AApeptide only leads to spherical nanoparticles (20–30 nm) under all concentrations tested. The size of the nanoparticles indicates these nanoparticles may be nanovesicles. We believe that because the removal of the amino groups leads to a decrease in electrostatic repulsion, now the vesicles are the most stable morphology. Under such circumstances, they do not aggregate or stack to form nanorods.

Although the intensive research to investigate different biological applications of  $\gamma$ -AApeptide amphiphiles will be carried out in the future, at the proof of concept, we studied the effect of  $\gamma$ -AA1 for the biomineralization of CaCO<sub>3</sub>. Calcium carbonate is the one of the most abundant biominerals, and its mineralization can be induced by proteins of many organisms.<sup>30</sup> It is a very important biological process because it is related to CO<sub>2</sub> storage and global warming. Therefore, the development of biomimetic ligands that can sequester CO<sub>2</sub> is of significant interest.<sup>31</sup> In the control, in which no  $\gamma$ -AA1 is present (Figure 8a), rhombohedral calcite crystals are mainly formed. Interestingly, in the presence of just 10  $\mu$ g/mL  $\gamma$ -AA1, the morphologies of the crystals are very different, and they tend to aggregate together. Although detailed study has to be carried out in the future, which is beyond the scope of this paper, the preliminary results demonstrated that  $\gamma$ -AApeptide amphiphiles can mimic natural proteins and control CaCO<sub>3</sub> nucleation and the growth of crystals.

## CONCLUSION

In summary, we have demonstrated that a biomimetic  $\gamma$ -AApeptide amphiphile can self-assemble into giant nanorods in a wide range of pHs. This is also the first report of  $\gamma$ -

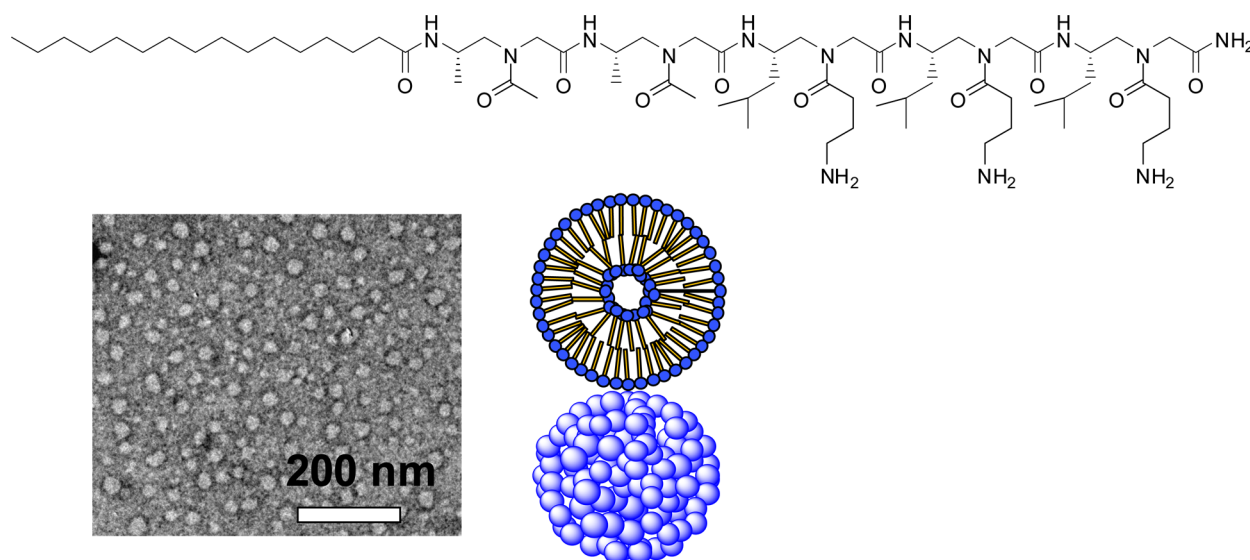


**Figure 7.**  $\gamma$ -AApeptide amphiphile  $\gamma$ -AA2 and its self-assembling nanoparticles. Top: chemical structure of  $\gamma$ -AA2. Bottom: TEM image of nanoparticles formed by the self-assembly of  $\gamma$ -AA2 in 0.5 mg/mL water solution.

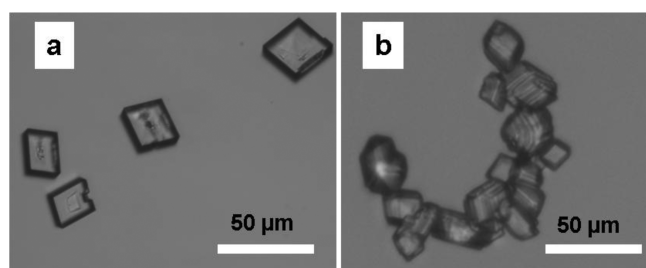


**Figure 8.** Morphology of  $\text{CaCO}_3$  crystals: (a) control, no  $\gamma$ -AA1; (b) in the presence of 10  $\mu\text{g}/\text{mL}$  of  $\gamma$ -AA1.

AApeptide-based nanomaterials. Because of the straightforward introduction of a wide variety of functional groups in AApeptides, there is enormous potential to generate  $\gamma$ -AApeptide nanomaterials with other nanostructures and desired functions. Such artificial peptide-based nanomaterials could enhance the current application of peptide-based amphiphiles by enriching the diversity of nanostructures so as to facilitate the application of material sciences. Meanwhile, the biocompatibility of  $\gamma$ -AApeptide could lead to novel biomimetic or bioinspired architectures for biological applications such as nanomedicine, drug delivery, and cell culture and tissue engineering in the future. Further exploration of the mechanistic formation of different types of nanostructures and extensive study for the rational design and application of  $\gamma$ -AApeptide-based nanomaterials are underway.

## ■ ASSOCIATED CONTENT

### ● Supporting Information

DLS, CD spectra, and characterization of  $\gamma$ -AApeptides. This material is available free of charge via the Internet at <http://pubs.acs.org>.

## ■ AUTHOR INFORMATION

### Corresponding Author

\*E-mail [Jianfengcai@usf.edu](mailto:Jianfengcai@usf.edu).

### Notes

The authors declare no competing financial interest.

## ■ ACKNOWLEDGMENTS

This work was supported by a USF start-up fund.

## ■ REFERENCES

- (1) Whitesides, G. M.; Grzybowski, B. *Science* **2002**, *295*, 2418–2421.
- (2) Versluis, F.; Marsden, H. R.; Kros, A. *Chem. Soc. Rev.* **2010**, *39*, 3434–3444.
- (3) Zhao, X. B.; Pan, F.; Xu, H.; Yaseen, M.; Shan, H. H.; Hauser, C. A. E.; Zhang, S. G.; Lu, J. R. *Chem. Soc. Rev.* **2010**, *39*, 3480–3498.
- (4) Ulijn, R. V.; Smith, A. M. *Chem. Soc. Rev.* **2008**, *37*, 664–675.
- (5) Cherny, I.; Gazit, E. *Angew. Chem., Int. Ed.* **2008**, *47*, 4062–4069.
- (6) Versluis, F.; Marsden, H. R.; Kros, A. *Chem. Soc. Rev.* **2010**, *39*, 3434–3444.
- (7) Zhao, X.; Nagai, Y.; Reeves, P. J.; Kiley, P.; Khorana, H. G.; Zhang, S. *Proc. Natl. Acad. Sci. U. S. A.* **2006**, *103*, 17707–17712.
- (8) Xu, H.; Wang, J.; Han, S.; Wang, J.; Yu, D.; Zhang, H.; Xia, D.; Zhao, X.; Waigh, T. A.; Lu, J. R. *Langmuir* **2009**, *25*, 4115–4123.
- (9) Vauthey, S.; Santoso, S.; Gong, H.; Watson, N.; Zhang, S. *Proc. Natl. Acad. Sci. U. S. A.* **2002**, *99*, 5355–5360.
- (10) Hartgerink, J. D.; Beniash, E.; Stupp, S. I. *Science* **2001**, *294*, 1684–1688.
- (11) Hartgerink, J. D.; Beniash, E.; Stupp, S. I. *Proc. Natl. Acad. Sci. U. S. A.* **2002**, *99*, 5133–5138.
- (12) Muraoka, T.; Koh, C. Y.; Cui, H.; Stupp, S. I. *Angew. Chem., Int. Ed.* **2009**, *48*, 5946–5949.
- (13) Cui, H.; Muraoka, T.; Cheetham, A. G.; Stupp, S. I. *Nano Lett.* **2009**, *9*, 945–951.
- (14) Kwon, S.; Jeon, A.; Yoo, S. H.; Chung, I. S.; Lee, H. S. *Angew. Chem., Int. Ed.* **2010**, *49*, 8232–8236.
- (15) Nam, K. T.; Shelby, S. A.; Choi, P. H.; Marciel, A. B.; Chen, R.; Tan, L.; Chu, T. K.; Mesch, R. A.; Lee, B. C.; Connolly, M. D.; Kisielowski, C.; Zuckermann, R. N. *Nat. Mater.* **2010**, *9*, 454–460.
- (16) Murnen, H. K.; Rosales, A. M.; Jaworski, J. N.; Segalman, R. A.; Zuckermann, R. N. *J. Am. Chem. Soc.* **2010**, *132*, 16112–16119.
- (17) Niu, Y.; Hu, Y.; Li, X.; Chen, J.; Cai, J. *New J. Chem.* **2011**, *35*, 542–545.
- (18) Wu, H.; Amin, M. N.; Niu, Y.; Qiao, Q.; Harfouch, N.; Nimer, A.; Cai, J. *Org. Lett.* **2012**, *14*, 3446–3449.
- (19) Niu, Y.; Padhee, S.; Wu, H.; Bai, G.; Harrington, L.; Burda, W. N.; Shaw, L. N.; Cao, C.; Cai, J. *Chem. Commun.* **2011**, *47*, 12197–12199.
- (20) Niu, Y.; Bai, G.; Wu, H.; Wang, R. E.; Qiao, Q.; Padhee, S.; Buzzeo, R.; Cao, C.; Cai, J. *Mol. Pharmaceutics* **2012**, *9*, 1529–1534.

- (21) Niu, Y.; Jones, A. J.; Wu, H.; Varani, G.; Cai, J. *Org. Biomol. Chem.* **2011**, *9*, 6604–6609.
- (22) Padhee, S.; Hu, Y.; Niu, Y.; Bai, G.; Wu, H.; Costanza, F.; West, L.; Harrington, L.; Shaw, L. N.; Cao, C.; Cai, J. *Chem. Commun.* **2011**, *47*, 9729–9731.
- (23) Wu, H.; Niu, Y.; Padhee, S.; Wang, R. E.; Li, Y.; Qiao, Q.; Ge, B.; Cao, C.; Cai, J. *Chem. Sci.* **2012**, *3*, 2570–2575.
- (24) Niu, Y.; Padhee, S.; Wu, H.; Bai, G.; Qiao, Q.; Hu, Y.; Harrington, L.; Burda, W. N.; Shaw, L. N.; Cao, C.; Cai, J. *J. Med. Chem.* **2012**, *55*, 4003–4009.
- (25) Bai, G.; Padhee, S.; Niu, Y.; Wang, R. E.; Qiao, Q.; Buzzeo, R.; Cao, C.; Cai, J. *Org. Biomol. Chem.* **2012**, *10*, 1149–1153.
- (26) Hu, Y.; Amin, M. N.; Padhee, S.; Wang, R.; Qiao, Q.; Ge, B.; Li, Y.; Mathew, A.; Cao, C.; Cai, J. *ACS Med. Chem. Lett.* **2012**, *3*, 683–686.
- (27) Lagant, P.; Vergoten, G.; Fleury, G.; Loucheux-Lefebvre, M. H. *Eur. J. Biochem.* **1984**, *139*, 137–148.
- (28) Frushour, B. G.; Koenig, J. L. *Biopolymers* **1975**, *14*, 363–377.
- (29) Mary, M. B.; Umadevi, M.; Pandiarajan, S.; Ramakrishnan, V. *Spectrochim. Acta, Part A* **2004**, *60*, 2643–2651.
- (30) Dey, A.; de With, G.; Sommerdijk, N. A. J. M. *Chem. Soc. Rev.* **2010**, *39*, 397–409.
- (31) Chen, C. L.; Qi, J. H.; Zuckermann, R. N.; DeYoreo, J. J. *J. Am. Chem. Soc.* **2011**, *133*, 5214–5217.